Patterned Biofunctional Poly(acrylic acid) Brushes on Silicon Surfaces

Rong Dong,[†,‡] Sitaraman Krishnan,[‡] Barbara A. Baird,[†] Manfred Lindau,[§] and Christopher K. Ober*[,‡]

Departments of Chemistry and Chemical Biology, Materials Science and Engineering, and Applied and Engineering Physics, Cornell University, Ithaca, New York 14853

Received May 6, 2007; Revised Manuscript Received July 11, 2007

Protein patterning was carried out using a simple procedure based on photolithography wherein the protein was not subjected to UV irradiation and high temperatures or contacted with denaturing solvents or strongly acidic or basic solutions. Self-assembled monolayers of poly(ethylene glycol) (PEG) on silicon surfaces were exposed to oxygen plasma through a patterned photoresist. The etched regions were back-filled with an initiator for surface-initiated atom transfer radical polymerization (ATRP). ATRP of sodium acrylate was readily achieved at room temperature in an aqueous medium. Protonation of the polymer resulted in patterned poly(acrylic acid) (PAA) brushes. A variety of biomolecules containing amino groups could be covalently tethered to the dense carboxyl groups of the brush, under relatively mild conditions. The PEG regions surrounding the PAA brush greatly reduced nonspecific adsorption. Avidin was covalently attached to PAA brushes, and biotin-tagged proteins could be immobilized through avidin−biotin interaction. Such an immobilization method, which is based on specific interactions, is expected to better retain protein functionality than direct covalent binding. Using biotin-tagged bovine serum albumin (BSA) as a model, a simple strategy was developed for immobilization of small biological molecules using BSA as linkages, while BSA can simultaneously block nonspecific interactions.

1. Introduction

The ability to pattern biomolecules, especially proteins, onto a substrate is important for a variety of biological studies and applications including biosensors, studies of cell-surface interactions, cell patterning, and the like.[1,2] Though concentrated efforts have been made on protein patterning, many methods are based on nonspecific physical adsorption on hydrophobic surfaces, wherein the proteins tend to unfold and partially denature[3] upon adsorption. The complexity of creating patterned substrates that combine self-assembled monolayers (SAMs) bearing functional groups to immobilize proteins with SAMs that are resistant to nonspecific protein adsorption leads to difficulties in effective surface construction. Veiseh et al. have created patterned surfaces containing both carboxylic acid groups and poly(ethylene glycol) (PEG) and used the surface for cell patterning studies.[4,5] In their work, it was necessary to use a gold-patterned silicon substrate and a combination of thiol−gold and silane chemistry to create the chemically patterned substrates. While the formation of SAMs of ω-mercapto carboxylic acids on gold-covered substrates is widely reported,[6−9] reports on direct functionalization of a silicon surface with carboxyl-terminated alkylchlorosilanes (or alkoxysilanes) are relatively rare. Some of the advantages of silicon surfaces are that they are inexpensive, molecularly flat, form thermally stable siloxy linkages with organosilanes, and are compatible with the well-established microfabrication techniques of the electronic industry. However, the fact that carboxyl-terminated alkylsilanes (which are required to form SAMs on silicon surfaces) are difficult to synthesize may have limited their use.[10] Moreover, strong interactions between the carboxyl head group of the silane and the silanol groups on the surface may complicate the process of SAM formation. To avoid this complication, vinyl-, carboalkoxy-, or bromo-terminated alkylsilanes have been converted to carboxylic acids after self-assembly and reaction with the surface silanol groups.[11−13]

Here we report the synthesis of poly(acrylic acid) (PAA) brushes by the atom transfer radical polymerization (ATRP) of sodium acrylate in aqueous media to generate carboxylic acid groups on a silicon surface. Besides providing a high surface density of −COOH groups for protein immobilization, the PAA brushes are expected to impart biocompatibility[14] and are more robust and self-healing toward defects than carboxyl-terminated SAMs. In comparison to carboxyl-terminated SAMs, PAA brushes have significantly higher protein-binding capacities due to high concentrations of −COOH groups at the brush interface.[15] Our synthetic methods enable the direct and efficient formation of PAA brushes in contrast to prior studies[15] that involved hydrolysis of poly(*tert*-butyl acrylate) brushes by means of strong acid catalysts and the use of potentially undesirable organic solvents.

We also describe the patterning of these PAA brushes using optical lithography as an effective alternative to microcontact printing. The creation of a patterned surface using multicomponent, microcontact printing (μCP) has become a widely used method. Usually, one compound is printed onto a substrate, and the patterned substrate is back-filled with another compound. The substrate used in μCP is often gold and not silicon, probably because the technique is more suited for thiol chemistry than the moisture-sensitive silane chemistry. In addition, depending on the nature and roughness of the stamp and substrate, defects of the monolayer are difficult to avoid in a large patterned area.

* Author to whom correspondence should be addressed. Phone: (607) 255-8417. Fax: (607) 255-2365. E-mail: cober@ccmr.cornell.edu.
† Department of Chemistry and Chemical Biology.
‡ Department of Materials Science and Engineering.
§ Department of Applied and Engineering Physics.

10.1021/bm700493v CCC: $37.00 © 2007 American Chemical Society
Published on Web 09/20/2007

Conventional photolithography also has been used previously to pattern multicomponent silanes on silicon surfaces.[1] A silicon surface may be first coated with a PEG monolayer prior to patterning a photoresist. After the photoresist is patterned, oxygen plasma cleaning may be used to etch the exposed PEG and also regenerate silanol groups on the etched surface to attach the surface initiator. Thus, Wang et al. have used photolithography to pattern PEG on a silicon surface and removed the exposed PEG via wet etching,[16] and Senaratne et al. used electron beam lithography to pattern a PEG monolayer on a silicon surface and back-filled the etched regions with organosilane molecules containing terminal dinitrophenyl groups.[17] While effective, electron beam lithography is expensive and time-consuming and not suitable for patterning large areas.

In this work, after a patterned PEGylated silicon surface was created using optical lithography, it was back-filled with a surface initiator for ATRP. PAA brushes were grown in the regions with tethered initiator molecules, by aqueous ATRP of sodium acrylate and subsequent formation of acid by rinsing with deionized water. As a proof of concept we demonstrate covalent immobilization of fluorescently labeled bovine serum albumin (BSA) onto PAA brushes yielding well-defined BSA patterns. We also demonstrate immobilization of biotin-tagged proteins through the avidin−biotin interaction by showing that fluoresceinated biotin can be immobilized onto a PAA brush region after avidin was attached to the brush. Furthermore, we look into the immobilization of small biological molecules onto PAA brushes using BSA as linkages. After biotinylated BSA was immobilized onto a PAA brush, the substrates were incubated with streptavidin and fluoresceinated biotin sequentially. Because BSA is a protein blocking agent, nonspecific adsorption of streptavidin onto the surface is further reduced. The binding of streptavidin is only due to the specific streptavidin−biotin interaction. This method can be extended to BSA tagged with other ligands, such as dinitrophenyl groups, to engineer spatially confined stimuli for the study of immunoglobulin receptor signaling. The avidin- or streptavidin-patterned surfaces may also be combined with ink-jet printing or nanoarray techniques for multiple protein patterning. The following section reviews prior methods of fabrication of carboxylate-functionalized surfaces.

1.1. Carboxylate-Functionalized Surfaces. The spontaneous reaction of amine-containing biomolecules with activated carboxylic acids makes silicon surfaces functionalized with carboxyl groups a versatile platform for microarray technology. A variety of biological molecules can be covalently immobilized on such substrates under mild conditions of pH and temperature. The use of silicon as a substrate allows the state-of-the-art approaches to the microfabrication of computer chips to be transferred to "biochip" production.[18,19] As noted above, reports of direct functionalization of silicon oxide surfaces with carboxylic acid groups remain relatively rare, and patterned carboxyl-functionalized surfaces are rarer still.

In an alternative approach to prepare carboxyl-functionalized silicon surfaces, Boukherroub et al. have used thermal hydrosilylation of ω-alkenyl carboxylic acid with a hydrogen-terminated silicon surface.[20] The same reaction was found to occur at room temperature when irradiated with 300 nm UV light.[21] Voicu et al. prepared DNA microarrays using photopatterning of undecylenic acid on a hydrogen-terminated silicon surface.[18] Irradiation of an air exposed Si−H surface through a patterned mask leads to the formation of oxide squares in the exposed regions. In a complex series of steps, the unexposed surface, consisting of Si−H groups, was reacted with ω-alkenyl carboxylic acid in the presence of UV light. The −COOH groups were then reacted with an amine-terminated PEG, and the PEGylated surface was immersed in an aqueous hydrofluoric acid solution to restore the Si−H groups in the oxide squares. These new silane groups were reacted with ω-alkenyl carboxylic acid under UV irradiation, and finally the −COOH groups in this region were activated with *N*-hydroxylsuccinimide (NHS) to bind DNA. Although an elegant method, a simpler procedure for micropatterning a silicon surface with −COOH and PEG groups would be desirable. More recently, Asanuma et al. have noted that the carboxyl groups could themselves react with hydrogen-terminated silicon, instead of the terminal $-CH{=}CH_2$ group,[22,23] necessitating the use of an ester-terminated alkene followed by deprotection of the carboxyl group after SAM formation. Alternative methods to prepare silicon surfaces that are densely functionalized with carboxyl groups will be quite useful.

1.2. Protein Patterning. The spatially defined presentation of a protein or biochemical ligand of interest against a protein-resistant background is of importance in several areas of biotechnology and biomedical research,[24] for example, in the design of supports for immobilizing antigens or antibodies in enzyme-linked immunosorbent assays (ELISA). Patterned arrays of carboxylated and PEGylated regions are useful for this purpose. The −COOH groups can be readily activated by forming acyl chlorides and nitrophenyl or succinimide esters, which undergo spontaneous reaction with the amine groups in a protein (N-terminal or ϵ-amino groups of lysine).[5,21] PEG is used to prevent nonspecific protein adsorption.[25−27] Potential advantages of dense microarrays in the field of genomics and proteomics have been discussed by Bhatnagar et al.[28] These include reduction in the volumes of analyte and reagents and higher signal-to-noise ratios. The basic criterion in the design of a protein microarray is that the protein must retain its native conformation (and hence its biological activity) after immobilization. Thus, the use of harsh solvents, strongly acidic or basic buffers, and exposure to UV and high temperatures are all undesirable.[29] Several methods have been used to micropattern proteins on surfaces, as discussed in the reviews by Blawas and Reichert[1] and Kane et al.[2]

López et al. have patterned a gold surface with methyl-terminated and PEGylated SAMs and have used physical adsorption of proteins on the hydrophobic methyl-terminated regions.[30] Physisorption of a protein on a surface is predominantly driven by hydrophobic interactions, especially in aqueous solutions of high ionic strengths. In the absence of competing proteins the adsorption is essentially irreversible. However, many proteins lose their native solution conformation, and hence activity, upon immobilization on a hydrophobic surface.[31] Physical adsorption on untreated glass has been used to pattern albumin,[32] but in high ionic strength buffers where electrostatic interactions are weak, desorption of the protein from the hydrophilic glass substrate is very likely. Covalent immobilization on hydrophilic substrates, as discussed by Lahiri et al.,[8,33] is more desirable.[34]

Photochemical techniques involving aryl azide chemistry, nitrobenzyl caging chemistry, and diazirine chemistry have also been used,[1] but these methods involve potentially denaturing UV irradiation of the protein. Sorribas et al. have used a UV lithography process, wherein a protein-immobilized surface is first covered by a protective sucrose layer, cured in an oven, spin-coated with a photoresist, irradiated with UV using a lithographic mask, developed to remove exposed photoresist, and treated with oxygen plasma to remove the protein from the exposed region.[35] The sucrose layer is believed to protect the

protein from organic solvents and alkaline solutions used in the process, which would otherwise denature the protein. Similarly, Lee et al. have used agarose as a protective layer in photolithographic patterning of proteins.[36] In addition, they have discussed the problems associated with microcontact printing, polydimethylsiloxane-based microfluidic systems, and the parylene-based peel-off process for direct patterning of proteins.

Jun et al. have formed patterns of HO- and CH_3O-terminated PEG regions on chlorine-terminated silicon surfaces using the soft lithographic techniques of microcontact printing and micromolding in capillaries (MIMIC).[37] The HO-terminated PEG regions were activated by either oxidation to aldehyde or using *N*,*N*′-disuccinimidyl carbonate, followed by covalent immobilization of protein molecules. The MIMIC technique has also found application in the work of Delamarche et al.[38] and Patel et al.[39]

Protein patterning on a sub-micrometer length scale has been achieved using electron beam lithography of organosilane SAMs[28,40] and surfaces of block copolymers as templates.[41] Zhang et al. created patterns of biotin in a hydrophobic perfluoroalkyl background but could avoid nonspecific adsorption by incubating the patterned surface with streptavidin for only a short time.[40]

In this paper we describe immobilization of proteins on patterned hydrophilic PAA brushes through covalent binding and avidin−biotin interaction. UV lithography was used to pattern a silicon surface covered with a PEGylated SAM. An initiator for ATRP was then attached to regions not covered by PEG. ATRP of sodium acrylate in water at or near room temperature, using the surface-tethered initiator, resulted in facile formation of patterned polymer brushes that were used to selectively immobilize fluorescently labeled proteins. The patterned proteins showed a sharp contrast against a protein-resistant PEG background when observed under a fluorescence microscope.

2. Experimental Section

2.1. Materials. Allyl 2-bromo-2-methylpropionate (CAS no. 40630-82-8, 98%), chlorodimethylhydrosilane (CAS no. 1066-35-9, 98%), Pt on activated carbon (10 wt %), triethylamine (CAS no. 121-44-8, 99.5%), sodium acrylate (CAS no. 7446-81-3, 97%), CuBr (CAS no. 7787-70-4, 99.999%), $CuBr_2$ (CAS no. 7789-45-9, 99.999%), 2,2′-bipyridine (CAS no. 366-18-7, ≥ 99%), *N*-hydroxylsuccinimide (NHS, CAS no. 6066-82-6, 98%), *N*-(3-dimethylaminopropyl)-*N*′-ethylcarbodiimide hydrochloride (EDC, CAS no. 25952-53-8, ≥ 98%), egg white avidin, bovine serum albumin labeled with fluorescein isothiocyanate (BSA−FITC), biotin-tagged bovine serum albumin (BSA−biotin, 8−16 mol biotin per mol albumin), streptavidin (from *Streptomyces*), 5(6)-(biotinamidohexanoylamido)pentylthioureidylfluorescein (fluorescein-tagged biotin, CAS no. 134759-22-1, ≥ 90%), phosphate-buffered saline (PBS) tablets, and 4-morpholineethanesulfonic acid (MES, CAS no. 4432-31-9, ≥ 99%) were purchased from Sigma-Aldrich and used without further purification. 2-[Methoxy(polyethylenoxy)propyl]-trichlorosilane (PEGylated silane, $CH_3O(CH_2CH_2O)_{6-9}(CH_2)_3SiCl_3$, 90%) was purchased from Gelest. Anhydrous toluene (99.8%) was purchased from Acros. All of the other solvents for rinsing and cleaning were obtained from Fisher. The PBS buffer solution was prepared by dissolving the PBS tablet in water to yield 0.01 M phosphate buffer, 0.0027 M potassium chloride, 0.137 M sodium chloride, and a pH of 7.4 at 25 °C. A MES solution of 50 mM concentration was prepared in water. The pH of this solution was 3.8.[42] The MES buffer solution was prepared by dissolving MES (50 mM) and NaOH (3 mM) in water to obtain a pH of about 5. Distilled deionized water and ultrapure nitrogen (99.99%, Airgas) were used throughout.

2.2. Patterning of PEG on a Silicon Wafer. Silicon wafers, rinsed with acetone and blown dry under nitrogen gas, were cleaned with oxygen plasma cleaner (Harrick Scientific) for 5 min. Self-assembled monolayers of PEG were prepared by the solution deposition technique. The silicon wafers were immersed in a 1% (v/v) solution of the PEGylated silane in anhydrous toluene containing catalytic amounts of triethylamine for about 12 h at room temperature, followed by rinsing with anhydrous ethanol and drying with nitrogen. After deposition, the substrates were baked at 115 °C for 10 min. S1813 positive tone photoresist (Shipley) was spin-coated onto the PEG-functionalized silicon wafers at 4000 rpm for 30 s and soft-baked at 115 °C for 1 min, resulting in a film about 1 μm thick. The wafer was then exposed to UV light (λ = 405 nm, 17 mW/cm^2) passed through patterns of lines with widths of 2 or 5 μm, for 2 s using a HTG System III-HR contact aligner. After development in a tetra-methyl ammonium hydroxide solution (AZ 300 MIF), the exposed PEG regions were etched using oxygen plasma. The remaining photoresist was stripped off using acetone, resulting in PEG stripes on a silicon surface. The PEG-patterned surfaces were used immediately in the next step of attaching the ATRP initiator.

2.3. Synthesis of the Surface Initiator and Immobilization of the Initiator. Hydrosilylation of allyl 2-bromo-2-methylpropionate was carried out using a literature procedure to obtain the ATRP initiator, 3-(chlorodimethylsilyl)propyl 2-bromo-2-methylpropionate (CAS no. 370870-81-8, cf. **1** in Scheme 2).[43] The PEG-patterned silicon substrates were immersed in a toluene solution of the initiator (5 mM) and triethylamine (0.05 mM) for 18 h. The wafers were then removed from the solution and washed with ethanol, water, and acetone sequentially. They were blown dry under nitrogen gas and used for surface-initiated polymerization. Plain silicon substrates without patterned PEG were similarly modified with the ATRP initiator.

2.4. Surface-Initiated Polymerization of Sodium Acrylate. The substrates (1 cm × 1 cm) were placed in a dry Schlenk flask. The flask was evacuated and back-filled with nitrogen three times. Sodium acrylate (1.88 g, 20 mmol), CuBr (57.4 mg, 0.4 mmol), $CuBr_2$ (9.0 mg, 0.04 mmol), and 2,2′-bipyridine (137.4 mg, 0.88 mmol) were added to another 25 mL Schlenk flask equipped with a magnetic stir bar. Air in this flask was evacuated and replaced with nitrogen three times. Four milliliters of water, which was purged with nitrogen for at least 30 min, was transferred to the Schlenk flask containing the monomer using a cannula. The mixture was stirred at room temperature under nitrogen for about 10 min until a brown solution was obtained. The solution was then transferred into the Schlenk flask containing the patterned substrates using a cannula. Polymerization was carried out at 30 °C for 2 h, after which the substrates were taken out of the solution and gently sonicated in a water−ethanol mixture for 5 min. They were then rinsed with water and ethanol, blown dry under nitrogen gas, and characterized by atomic force microscopy (AFM). Unpatterned polymer brushes on silicon were characterized by ellipsometry and X-ray photoelectron spectroscopy (XPS).

2.5. Immobilization of BSA−FITC. The wafers (1 cm × 1 cm) with a patterned PEG SAM and PAA brushes were immersed in 5 mL of MES solution (50 mM, pH ≈ 3.8) containing EDC (40 mg) and NHS (24 mg). After 10 min, the substrates were taken out of the solution, rinsed with MES buffer, and covered with a 100 μg/mL solution of BSA−FITC in MES buffer solution (pH ≈ 5.0). After 1 h of incubation in darkness, the substrates were thoroughly rinsed and left in PBS buffer solution (pH ≈ 7.4) overnight to deactivate unreacted NHS ester.

2.6. Immobilization of Avidin and Incubation with Fluoresceinated Biotin. Avidin was immobilized on PEG−PAA-patterned silicon surfaces as described in subsection 2.5, but a 100 μg/mL solution of avidin in MES buffer solution (pH ≈ 5.0) was used instead of BSA−FITC. The protein-immobilized surface was incubated in a solution of 100 μg/mL fluoresceinated biotin in a PBS buffer solution, in the dark for 1 h. Finally, the substrates were washed with PBS buffer solution (pH ≈ 7.4) and observed under a fluorescence microscope. A PEG−

Scheme 1. Patterning of PEG and PAA Brushes on Silicon Surface[a]

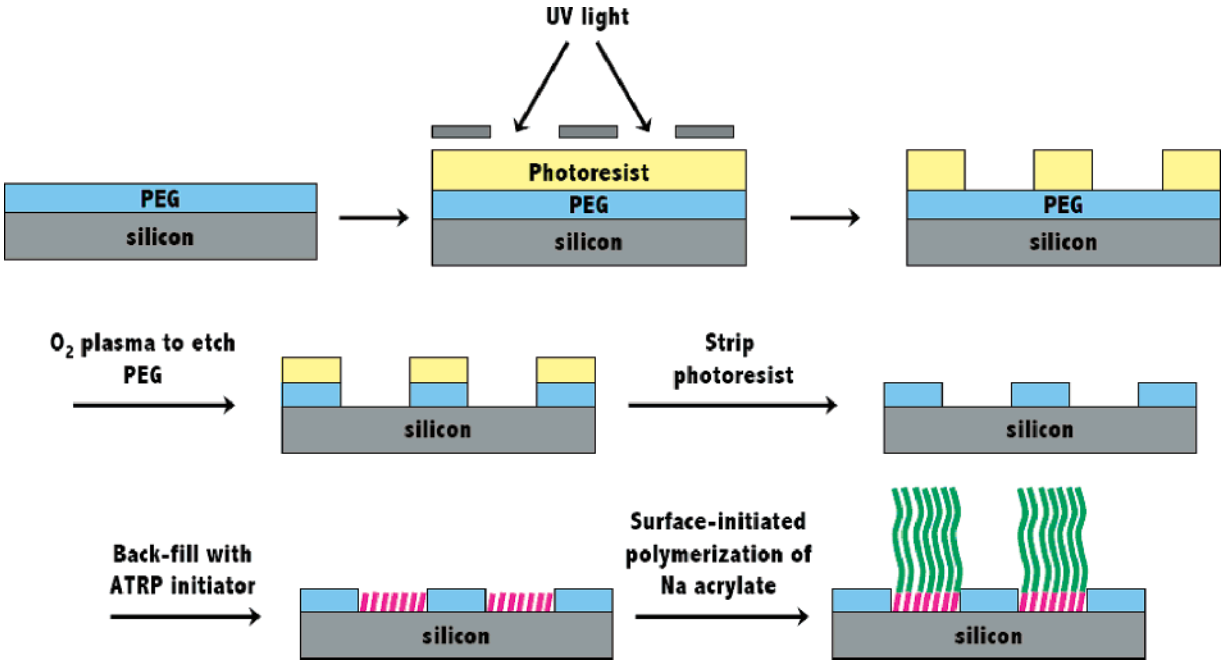

[a] Not to scale.

Scheme 2. Surface-Initiated Polymerization of Sodium Acrylate Using ATRP

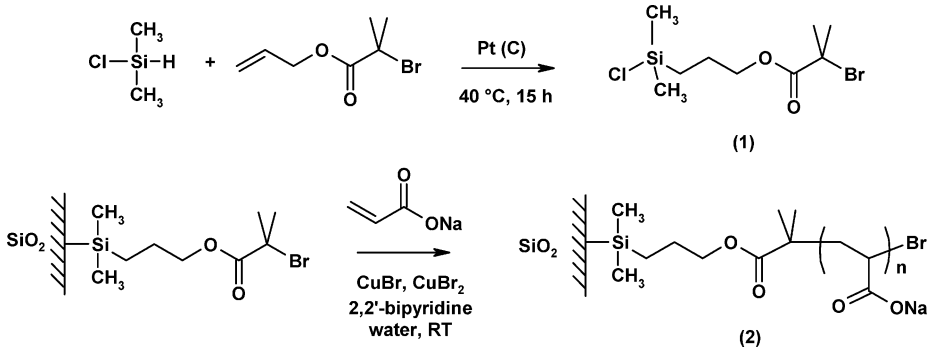

PAA-patterned substrate without avidin was incubated with fluoresceinated biotin in PBS buffer solution for an hour and used as a control. Avidin was also immobilized onto nonpatterned PAA brush surfaces. These surfaces were then characterized by XPS.

2.7. Immobilization of BSA−Biotin and Making a Biotin−Streptavidin−Biotin Sandwich. Biotinylated BSA was immobilized onto PAA brushes of the PEG−PAA-patterned substrates using EDC/NHS-mediated coupling, as described in subsection 2.5. A 100 μg/mL solution of the protein in MES buffer solution (pH $\approx$ 5.0) was used. The BSA−biotin-functionalized substrates were incubated with 100 μg/mL of streptavidin in a PBS buffer solution (pH $\approx$ 7.4) for 1 h. After being rinsed several times to remove free streptavidin, the substrates were incubated with a 100 μg/mL solution of fluoresceinated biotin (in PBS buffer solution), in the dark for 1 h. The substrates were finally rinsed with PBS buffer solution and imaged under a fluorescence microscope. The control surfaces were prepared in an identical manner, except that BSA was used instead of biotinylated BSA.

2.8. X-ray Photoelectron Spectroscopy. XPS measurements were performed using a Kratos Axis Ultra Spectrometer (Kratos Analytical, Manchester, U. K.) with a monochromatic Al Kα X-ray source (1486.6 eV) operating at 280 W (14 kV, 20 mA). Charge neutralization was carried out by injection of low-energy electrons, and the C−C 1s peak was corrected to a binding energy of 285 eV. The pass energy of the analyzer was set at 20 eV for high-resolution spectra and 80 eV for survey scans, and data were acquired at energy steps of 0.5 and 0.1 eV, respectively. The high-resolution spectra were fitted using a Tougaard background and Gaussian−Lorentzian (sum) line shapes for subpeaks.

2.9. Fluorescence Microscopy. Fluorescence microscopy was performed using an Olympus BX51 upright microscope with a 40× UPlan Fluorite 40× dry objective (N.A. 0.75). Images were acquired using a Roper CoolSnap HQ CCD camera and Image Pro image acquisition and processing software. Fluorescein and FITC were observed with a 450 nm excitation and 550 nm emission filter set. False color fluorescence images reported here were processed using the ImageJ 1.36b software. All sets of control and test images were processed in an identical manner. Moreover, representative line sections of as-obtained and unprocessed images are also shown to compare fluorescence intensity from different parts of the patterned surfaces.

2.10. Contact Angles, Surface Topography, and Film Thickness. Contact angles were measured using a Naval Research Laboratories contact angle goniometer (Ramé-Hart Model 100-00) at room temperature. Dynamic water contact angle measurements were performed by addition and retraction of a drop of water on the surface. Surface topography and roughness were determined using a Veeco Dimension 3100 scanning probe microscope in the tapping mode. Thicknesses of the PEG layer and the PAA brush were measured by a Woollam variable angle spectroscopic ellipsometer at a 70° angle of incidence. A Cauchy model (Cauchy layer/silicon substrate) was used to fit the data, in which the Cauchy layer was representative of the PEG SAM or the PAA brush.

3. Results and Discussion

3.1. PEG−PAA-Patterned Surfaces. The overall procedure for forming PEG−PAA patterns on a silicon substrate is shown in Scheme 1. Ellipsometry showed that the thickness of the PEG layer was about 2.2 nm. Photolithography was used in this study to create patterns of a PEG SAM on silicon; however, the patterned PEG surface can also be prepared by other techniques such as microcontact printing or electron beam lithography. The siloxane bonds at the SAM−silicon interface are relatively stable and withstand the high temperatures (~115 °C) involved in the patterning process. The regions not covered by the PEG were back-filled with the ATRP initiator. PAA brushes were grown by ATRP at room temperature.

3.2. PAA Brushes. Due to the possibility of interaction of the carboxylic acid groups with the ATRP catalyst,[44] PAA is usually prepared by hydrolysis of poly(*tert*-butyl acrylate).[45] Matyjaszewski et al. have reported an ATRP synthesis of polystyrene-*block*-poly(*tert*-butyl acrylate) brushes on silicon surfaces, which were converted to polystyrene-*block*-poly(acrylic acid) by refluxing the surfaces in aqueous hydrochloric acid solution.[46] Similarly, Kurosawa et al. have prepared PAA brushes by plasma polymerization of allyl alcohol on a quartz surface, reaction of the surface −OH groups with 2-bromo-2-methylpropionyl bromide, growth of *tert*-butyl acrylate brushes by ATRP, and conversion of the *tert*-butyl acrylate groups to acrylic acid by refluxing with trifluoroacetic acid in dichloromethane.[47] However, this method is problematic if the surface bound initiator also contains an ester group, which can also undergo hydrolysis resulting in removal of the polymer chains from the surface. Treat and co-workers have recently reported the formation of PAA brushes by high-temperature deprotection of poly(*tert*-butyl acrylate).[48] Pyrolysis of the *tert*-butyl ester at 200 °C for 30 min produced carboxylic acid with isobutylene as a side product. However, this procedure may not be compatible with our strategy shown in Scheme 1. The pyrolysis may have undesirable effects on the PEG SAMs.

Ashford et al. observed that aqueous ATRP of sodium methacrylate resulted in controlled molecular weights and narrow molecular weight distributions.[49] Osborne and co-workers have also prepared triblock copolymer brushes containing a poly(methacrylic acid) block by aqueous ATRP of sodium methacrylate.[50] Grazing incidence Fourier transform infrared spectra showed that rinsing the brush surface with water protonated the anion and removed the Na^+ ions from the brush.

We have found that ATRP growth of sodium acrylate brushes may be successfully performed in water at room temperature using the CuBr/2,2′-bipyridine catalyst system. Reactions for the synthesis of surface-initiated ATRP initiator, 3-(chlorodimethylsilyl)propyl 2-bromo-2-methylpropionate, and the PAA brushes are shown in Scheme 2. About 10% of $CuBr_2$ (relative to CuBr) was used to moderate the polymerization rate. X-ray photoelectron spectra revealed the absence of Na^+,[51] suggesting that the carboxylate anions were fully protonated. XPS studies also indicated the absence of CuBr or $CuBr_2$ at the brush surface.[52] The advancing and receding water contact angles of the PAA brush surface were $\theta_{AW} = 45°$ and $\theta_{RW} = 9°$, respectively. Treat et al. have reported $\theta_{AW} = 48°$ and $\theta_{RW} = 34°$,[48] while Husemann et al. observed an advancing water contact angle of 15°.[53] If the brush thicknesses are comparable, then the reason for the differences in contact angles must lie in the thermal and solvent treatments of the brushes before contact angle measurements. The brush surface was rinsed with water and ethanol and dried at room temperature in a vacuum oven before measuring the contact angles. Both ellipsometry and AFM (Figure 1) showed that the dry thickness of the PAA brushes was about 30 nm.

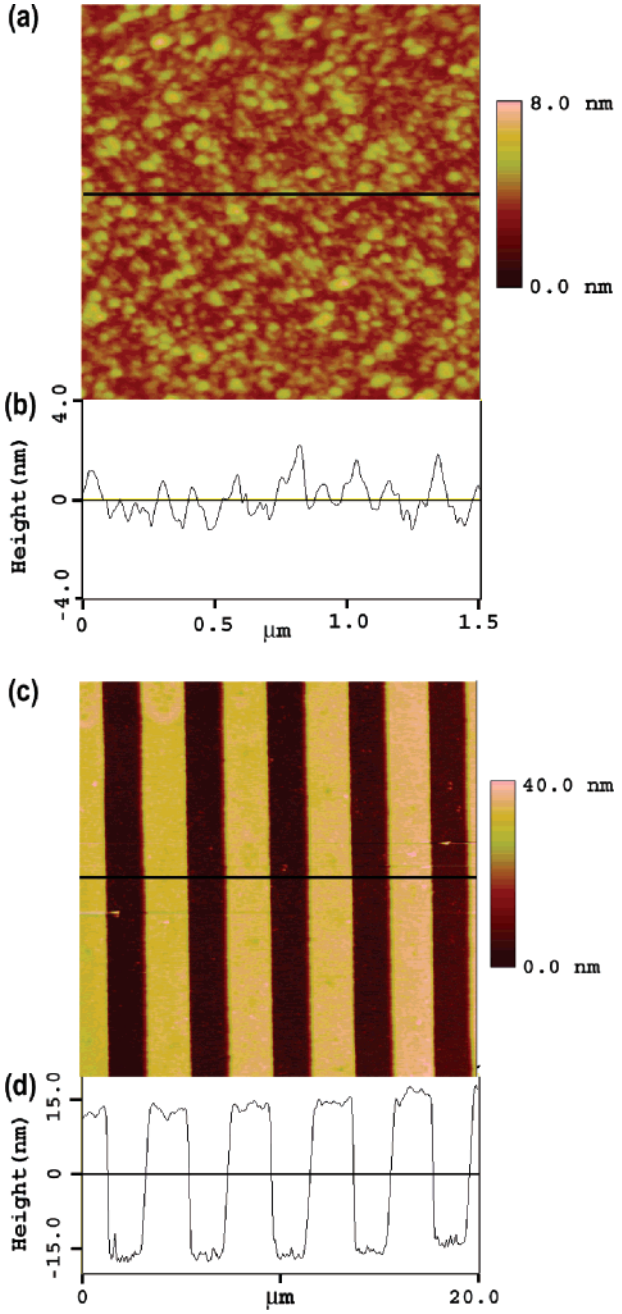

Figure 1. Tapping-mode scanning probe microscopy height images of (a) a PAA brush grown by surface-initiated polymerization and (c) 2-μm-wide alternating stripes of a PEG SAM and PAA brush on silicon substrates. The height profiles of transverse sections near the centers of the scan regions are shown in panels b and d, respectively.

Figure 1a shows a height image of a PAA brush surface obtained by scanning probe microscopy. The surface was rinsed with ethanol after polymerization and dried under a stream of nitrogen at room temperature. The root-mean-square roughness was 0.7 nm. The height image of a patterned silicon surface with 2-μm-wide PAA stripes juxtaposed to PEG-covered stripes is shown in Figure 1b. The ATRP initiator selectively attached to regions not covered by PEG and could successfully initiate polymerization of the sodium acrylate monomer. The surface composition of the PAA brush was characterized using X-ray photoelectron spectroscopy. The C 1s peak could be deconvoluted into three subpeaks positioned at binding energy values

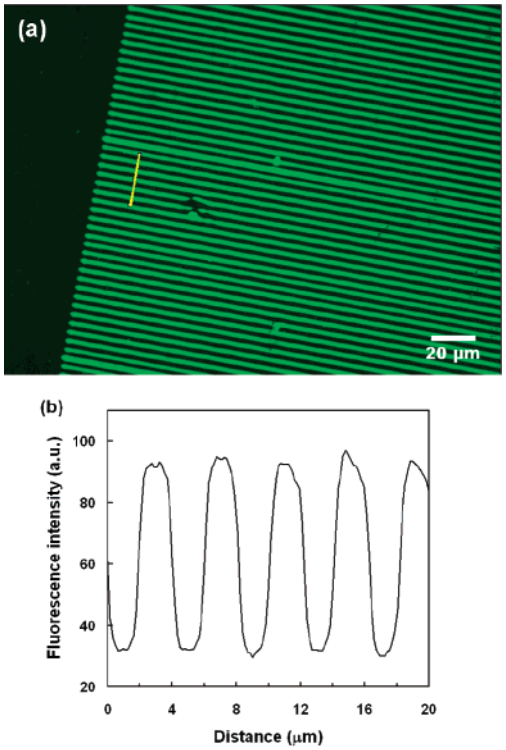

Figure 2. (a) Fluorescence image of BSA−FITC immobilized on 2-μm-wide PAA brush patterns in a background consisting of PEG SAM (cf. Scheme 3). The darker regions are the PEG-covered substrate where there was no covalent binding or nonspecific adsorption of BSA−FITC. (b) Intensity profile along a line section shown in panel a.

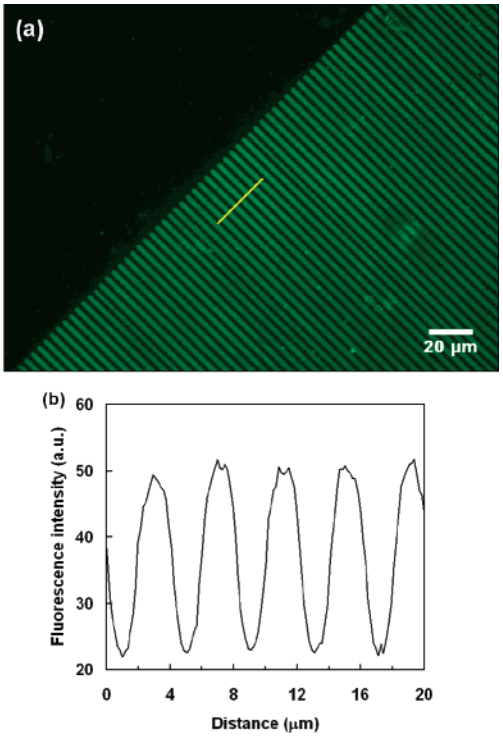

Figure 3. (a) Fluorescence microscopy image of avidin-immobilized PEG−PAA-patterned surface that was incubated with fluoresceinated biotin (cf. Scheme 4) and (b) intensity profile along a line section shown in panel a.

of 285, 285.4, and 288.8 eV, and with relative areas of 42%, 29%, and 29%, respectively (cf. Supporting Information). The curve-fitting results are in accord with previously reported XPS characterization of PAA surfaces.[54] The PEG SAM showed two peaks, at 286.5 and 285 eV, respectively. The former peak, with a relative area of 87%, corresponds to the ether carbon atoms of the PEG group. The hydrocarbon peak arises from the propyl carbon atoms in the PEGylated molecules used for preparing the SAM.

3.3. Protein Patterning through Covalent Immobilization. The patterned PAA brushes were further characterized using the binding of fluorescently labeled BSA. Figure 2 is a fluorescence image of a pattern with 2-μm-wide stripes of PAA in a PEGylated background. BSA−FITC was selectively immobilized on the PAA regions resulting in fluorescence, while the PEG regions were dark. The fluorescence intensity did not change significantly even after washing with 0.5 M sodium chloride solution in water, indicating that protein immobilization on the PAA brush was very stable.[55]

Covalent immobilization of proteins on the PAA brush was carried out as shown in Scheme 3 using a published procedure.[8,56] Activated NHS esters of the polymer carboxylic acids were first generated by a reaction mediated by the water-soluble carbodiimide, EDC. The reaction was performed in 50 mM MES solution (pH $\approx$ 3.8). The NHS esters were then reacted with ϵ-amino groups of lysine residues in a MES buffer solution (pH $\approx$ 5.0). After immobilization, the surfaces were washed and incubated with a PBS buffer solution (pH $\approx$ 7.4) to hydrolyze residual NHS esters.

Lahiri et al. have found that the highest levels of protein immobilization were obtained when the pH of the coupling buffer was one unit below the pI of the protein, that is, when the protein was positively charged.[8] A favorable electrostatic interaction between the positively charged protein and the negatively charged carboxylate group was hypothesized to be responsible for this effect. However, they have also noted certain ambiguities in this hypothesis. Because the carboxylic acid groups were quantitatively converted to NHS esters before protein coupling, the surface is expected to be largely neutral in the ester form. But it is likely that the hydrolysis of the NHS ester is fast relative to the coupling of the protein, in which case the surface would be negatively charged. Moreover, protonation of the ϵ-amino groups of lysine residues is of concern at lower values of pH. The reduced nucleophilicity due to protonation is unfavorable for the coupling reaction. Nevertheless, Lahiri et al. have achieved immobilization of a variety of proteins in solutions with pH values of 7 or lower. The ϵ-amino groups of the lysine have a pK_a of 10.4.[57] Therefore, almost all of the $-NH_2$ groups are expected to be protonated at these pH values. Yet, significant amounts of proteins attached to the carboxylated surfaces. We used a MES buffer solution of pH $\approx$ 5.0 for immobilizing both BSA (pI = 4.9) and avidin (pI = 10.8). Initial experiments using fluorescence microscopy showed that acidic media resulted in higher amounts of BSA immobilization (data not shown). We also used XPS to characterize the BSA immobilization onto unpatterned PAA brushes on a silicon surface (cf. Supporting Information). About 80% of the carbon atoms at the surface belonged to protein molecules, which is indicative of the high surface coverage that can be achieved using this method.

3.4. Protein Patterning Using Avidin−Biotin Affinity. In subsection 3.3, we discussed covalent immobilization of BSA on PAA brushes. Although the covalent binding method is simple and provides stable immobilization, it usually involves a multipoint attachment of proteins to surfaces, resulting in a random orientation of the immobilized protein and a loss of activity associated with structural deformation.[58] Single-point attachment of proteins is expected to result in a more controlled

Scheme 3. Protein Immobilization on a PAA Brush Surface by EDC/NHS Coupling

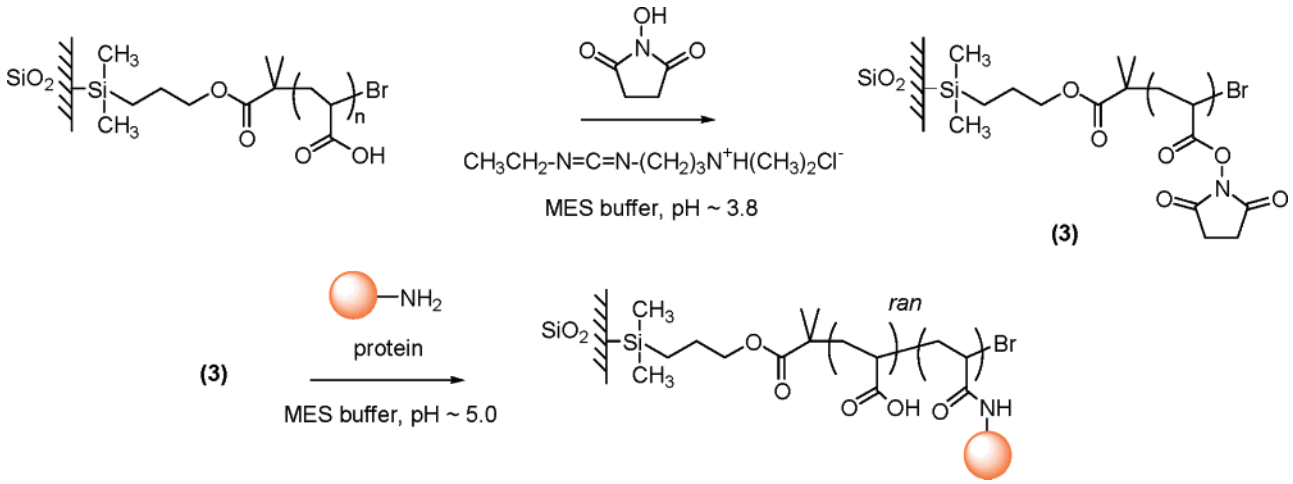

Scheme 4. Protein Immobilization to PAA Brushes through Avidin−Biotin Interaction

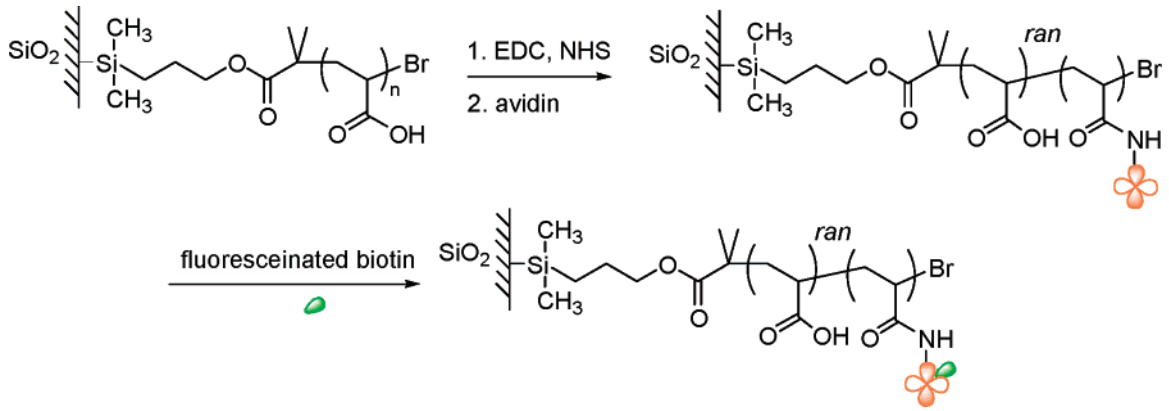

and oriented immobilization. The avidin−biotin interaction is widely used for controlled immobilization of proteins. Because each avidin molecule has four biotin-binding sites, avidin−biotin complex formation also has been used for multilayer immobilization of proteins and enzymes.[59] Here, we created patterned arrays of avidin, on a PEGylated background, for further functionalization with biotinylated molecules. Avidin was covalently attached to PAA brushes through EDC/NHS coupling. Biotin-tagged proteins may then be immobilized onto the surface through avidin−biotin interaction, which was demonstrated by attachment of fluoresceinated biotin to avidin modified regions, as shown in Scheme 4.

The attachment of avidin to the PAA brush was confirmed by fluorescence microscopy. The binding of fluorescein-tagged biotin to avidin[60] resulted in the image shown in Figure 3. The control surface, where the PEG−PAA-patterned surfaces were incubated with fluorescein-labeled biotin, showed negligible binding of biotin (data not shown).

X-ray photoelectron spectroscopy was used to characterize the binding of avidin to unpatterned PAA brushes. Figure 4a shows the XPS survey scan of a PAA brush surface with immobilized avidin, which is qualitatively similar to the XPS spectrum of avidin reported by Nehilla et al.[61] We carried out a detailed analysis of the high-resolution C 1s spectrum to determine the extent of attachment of avidin to the PAA brush. Avidin is a well-characterized glycoprotein and is amenable to such an analysis. It consists of four identical polypeptide chains, each containing about 128 amino acid residues.[62] Each subunit has a carbohydrate moiety attached at the asparaginyl residue 17 (Asn_{17}). The oligosaccharides attached to the four subunits can be compositionally different but contain, on average, 5 mannose and 3 *N*-acetylglucosamine moieties per subunit.[63]

Figure 4b shows a high-resolution C 1s XPS spectrum of an avidin−PAA surface. Deconvolution of the C 1s peak into subpeaks was performed on the basis of high-resolution C 1s XPS spectra of model poly(amino acid) surfaces reported by Bomben and Dev.[64] Using a series of homopolymeric amino acids, Bomben and Dev found that deconvolution of the C 1s peak into only three subpeaks, corresponding to the C−C or C−H hydrocarbon peak at 285.0 eV, the amide C═O peak at 287.8 eV, and the amine C−N peak at 286.3 eV, resulted in good agreement between the experimental ratios of peak areas and the theoretical ratios. The theoretical areas of peaks were calculated from the known poly(amino acid) structure. The use of more than three peaks was not found to be necessary. However, the hydroxylated amino acids, threonine (Thr) and serine (Ser), were not studied by Bomben and Dev. Avidin has a high content of these amino acids (20 Thr residues and 9 Ser residues per subunit). In fact, the fraction of Thr residues in avidin (~0.16) is higher than that of any other amino acid residue. Moreover, the oligosaccharides attached to Asn_{17} contain mannose and *N*-acetylglucosamine moieties, which are also highly hydroxylated. These oligosaccharides constitute about 10% of the total mass of the glycoprotein. Hence, in addition to the three characteristic poly(amino acid) peaks used by Bomben and Dev,[62] a C−O (alcohol or ether) peak is also expected near 286.5 eV in the XPS spectrum. In addition, a carboxylic acid C═O peak due to the PAA brush will be observed near 289 eV. As can be seen from Figure 4b, the experimental spectrum could be fitted very well (correlation

CDV

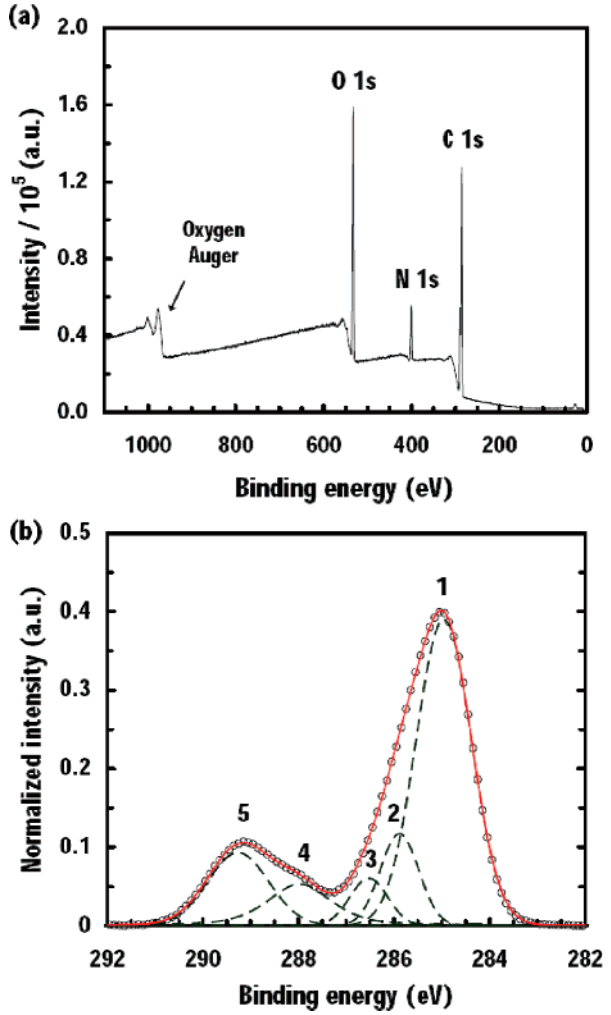

Figure 4. (a) XPS survey spectrum of covalently immobilized avidin on a PAA brush surface and (b) the high-resolution C 1s spectrum, resolved into component peaks. The peak assignments are: (1) C−C and C═C, (2) C−N and C═N, (3) C−OH and C−O−C, (4) C═O (amide), and (5) C═O (carboxylic acid). The circles represent the experimental data points. The continuous line is the best-fit curve. The dashed curves are fitted subpeaks. The spectra were acquired at an electron emission angle of 0°.

Table 1. Relative Areas of the C 1s Subpeaks in the XPS Spectrum of the Avidin-Tethered PAA Brush Surface and Number Distribution of Carbon Atoms at the Surface

			percentage of C 1s peak area		
peak	position (eV)	carbon atom	total	avidin	PAA
1	285.0	C−C and C═C	56.3	23.9	32.4
2	285.9	C−N and C═N	11.8	11.8	
3	286.5	C−O	6.0	6.0	
4	288.0	C═O (amide)	11.0	11.0	
5	289.3	C═O (acid)	14.9	1.0	13.9

coefficient, $r = 0.999$) using these five subpeaks.[65] Gauss−Lorenztian sums were used as the line shapes for curve fitting. Table 1 shows the peak positions and relative areas of the fitted subpeaks. Using the experimentally known ratios of C−C and C═O peak areas for PAA (from the C 1s XPS data for a PAA brush shown in the Supporting Information), the individual contributions of avidin and PAA to the peak areas were also calculated, as given in Table 1.

The relative areas of subpeaks shown in Table 1 are in good agreement with the known composition of avidin: C−C and C═C 44.48%, C−N and C═N 21.94%, C−O 10.90%, C═O (amide) 20.91%, and C═O (acid) 1.77%. The expected distribution of carbon atoms in avidin was calculated from its amino acid and oligosaccharide compositions as reported by DeLange and Huang.[62,66] These values are also in accord with the relative areas of C 1s subpeaks in the XPS spectrum of pure avidin (data not shown).

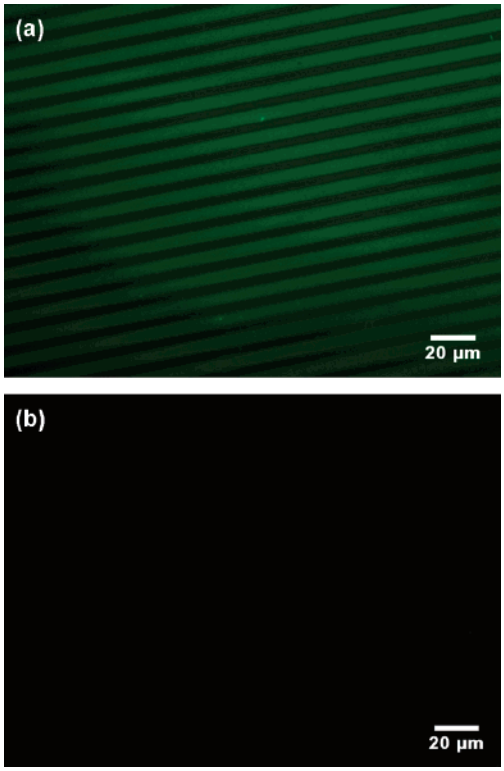

Figure 5. (a) Fluorescence microscopy image of a streptavidin-immobilized BSA−PAA surface that was incubated with fluoresceinated biotin. Immobilization of streptavidin was achieved through biotinylated BSA, which was covalently tethered to the PAA stripes (cf. Scheme 5). The darker regions correspond to PEG. (b) A control patterned surface where the BSA was not tagged with biotin. No streptavidin, and hence no fluoresceinated biotin, attached to the surface.

It is evident from the values reported in Table 1 that about 54% of the C 1s peak area is from avidin. The avidin molecules can be localized on the silicon surface in two distinctly different ways. First, they can form a monolayer on top of the PAA brush without diffusing into the brush. Second, they can penetrate the brush layer. For a monolayer of avidin with a thickness, d, of ~4.8 nm[67] and an electron escape depth, λ, of ~3.3 nm,[68] the expected contribution of avidin to the C 1s peak area is about 76.6%,[69] which is higher than the experimentally determined value of 54%. Thus, we have either less than complete coverage of avidin at the PAA surface or a situation where the protein molecules penetrate the PAA brush. Prior studies[70,71] have shown that protein molecules do not just bind to the surfaces of PAA brushes but can also penetrate and interact with the brush interior.[72]

3.5. Patterning Small Biological Molecules Using BSA as Linkages. In subsections 3.4 and 3.5, we discussed two methods to pattern proteins that have several functional groups available for modification with other biomolecules and ligands. A single molecule of BSA has about 60 lysine residues, and hence 60 amino groups that can react with carboxylic acids. Thus, BSA can function as a multisite linkage between biofunctional ligands, such as biotin or 2,4-dinitrophenyl moieties, and patterned PAA brushes. Moreover, BSA is commonly used to

Scheme 5. Immobilization of Biotin Using BSA as Linkages

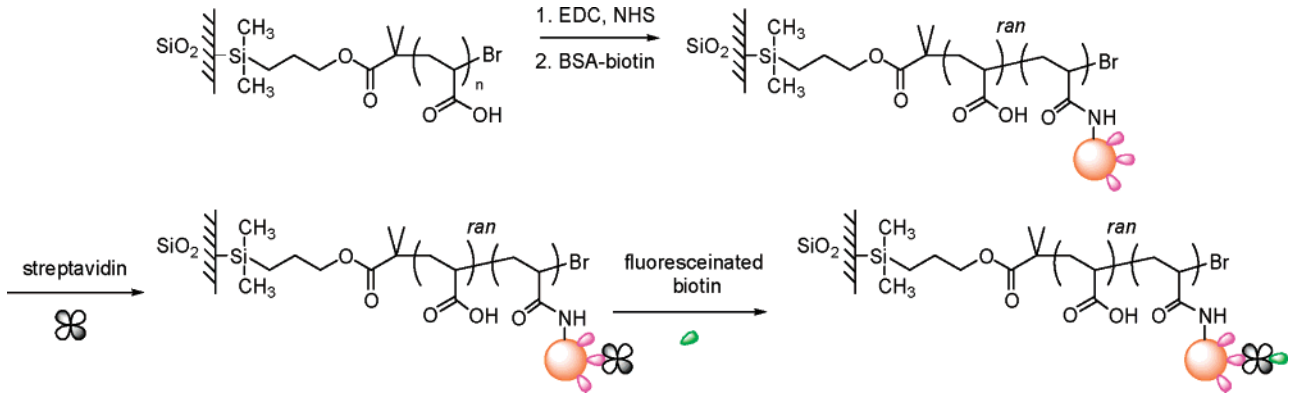

"block" nonspecific adsorption of biomolecules on surfaces.[73] Here, we used biotinylated BSA to pattern biotin molecules on silicon surfaces. The PAA regions were selectively functionalized with biotinylated BSA by covalent coupling. The surfaces were then incubated with a PBS buffer solution of streptavidin (pI $\approx$ 5.3). Biotin−streptavidin complex formation (affinity constant $\sim 10^{15}$ M^{-1}) resulted in an almost irreversible immobilization of streptavidin on the PAA regions. The streptavidin binding was characterized by complexation of fluoresceinated biotin with streptavidin. The series of reactions are represented in Scheme 5.

Figure 5a shows a fluorescence microscopy image of streptavidin immobilized on 5-μm-wide PAA brushes. The control experiment was carried out by covalently immobilizing BSA onto PEG−PAA-patterned surfaces, incubating the BSA-functionalized patterned surface with streptavidin, and finally incubating with biotin−fluorescein. It is evident from Figure 5b that there was no streptavidin attachment in the absence of biotin, which confirmed the specificity of streptavidin attachment onto the biotinylated patterns and showed that both BSA and PEG prevented the nonspecific adsorption of streptavidin. Such surfaces can minimize nonspecific interactions between biological molecules inside the patterned regions and the regions surrounding the patterns as well.

4. Conclusion

A versatile procedure was developed to pattern biological molecules with low-level nonspecific adsorptions. A PEG monolayer was patterned based on photolithography. Surface-initiated ATRP of sodium acrylate was carried out successfully in water at room temperature on patterned surfaces where PEG was etched. PAA brushes acted as robust templates for protein immobilization by providing a high density of −COOH groups on the surface, while PEG surrounding the brushes restricted proteins into the brush region further.

Two different strategies for protein immobilization were discussed. First, protein (BSA) molecules were directly immobilized on PAA brushes through covalent linkages. Second, a protein such as avidin was attached, which could then be used to bind different biotinylated molecules through the almost irreversible avidin−biotin interaction. We also used a simple strategy to immobilize small biological molecules using BSA as linkages. We have utilized the effectiveness of BSA in blocking nonspecific interactions by immobilizing biotin-tagged BSA to the patterned brushes. We found that the attachment of streptavidin was only through specific recognition of biotin. Streptavidin did not bind in the absence of the latter. Moreover, by itself being a polypeptide, BSA offers a nondenaturing environment for immobilizing other proteins. Thus, this method can be expanded to immobilize a range of antigens or ligands for biosensing applications and to study cell-surface interactions. The problem of nonspecific binding can be greatly reduced by this approach.

Acknowledgment. This research was supported by the National Science Foundation (NSF)-funded Nanoscale Interdisciplinary Research Team (NIRT) program (Grant No. ECS-0103297-NIRT), the Cornell Nanobiotechnology Center (NBTC) and the Office of Naval Research (ONR) (Grant No. N00014-02-1-0170). It made use of the facilities at the NBTC, the Cornell NanoScale Science and Technology Facility, and the Cornell Center for Materials Research, all of which are supported by the NSF. The NIRT and NBTC support for R.D. and the ONR support for S.K. are gratefully acknowledged. XPS spectra of the avidin-immobilized PAA surfaces were acquired by Robert W. Hengstebeck at the Materials Characterization Laboratory of the Pennsylvania State Univeristy.

Supporting Information Available. XPS spectra of a PAA brush, a PEG SAM, and BSA-tethered PAA brush surfaces. This material is available free of charge via the Internet at http://pubs.acs.org.

References and Notes

(1) Blawas, A. S.; Reichert, W. M. Protein patterning. *Biomaterials* **1998**, *19*, 595−609.
(2) Kane, R. S.; Takayama, S.; Ostuni, E.; Ingber, D. E.; Whitesides, G. M. Patterning proteins and cells using soft lithography. *Biomaterials* **1999**, *20*, 2363−2376.
(3) Seigel, R. R.; Harder, P.; Dahint, R.; Grunze, M.; Josse, F.; Mrksich, M.; Whitesides, G. M. On-line detection of nonspecific protein adsorption at artificial surfaces. *Anal. Chem.* **1997**, *69*, 3321−3328.
(4) Veiseh, M.; Zhang, Y.; Hinkley, K.; Zhang, M. Q. Two-dimensional protein micropatterning for sensor applications through chemical selectivity technique *Biomed. Microdevices* **2001**, *3*, 45−51.
(5) Veiseh, M.; Zhang, M. Effect of silicon oxidation on long-term cell selectivity of cell-patterned Au/SiO_2 platforms. *J. Am. Chem. Soc.* **2006**, *128*, 1197−1203.
(6) Nuzzo, R. G.; Dubois, L. H.; Allara, D. L. Fundamental studies of microscopic wetting on organic surfaces. 1. Formation and structural characterization of a self-consistent series of polyfunctional organic monolayers. *J. Am. Chem. Soc.* **1990**, *112*, 558−569.
(7) Malem, F.; Mandler. D.; Self-assembled monolayers in electoanalytical chemistry: Application of ω-mercapto carboxylic acid monolayers for the electrochemical detection of dopamine in the presence of high concentration of ascorbic acid. *Anal. Chem.* **1993**, *65*, 37−41.
(8) Lahiri, J.; Isaacs, L.; Tien, J.; Whitesides, G. M. A strategy for the generation of surfaces presenting ligands for studies of binding based on an active ester as a common reactive intermediate: A surface plasmon resonance study. *Anal. Chem.* **1999**, *71*, 777−790.

(9) Ista, L. K.; Callow, M. E.; Finlay, J. A.; Coleman, S. E.; Nolasco, A. C.; Simons, R. H.; Callow, J. A.; Lopez, G. P. Effect of substratum surface chemistry and surface energy on attachment of marine bacteria and algal spores. *Appl. Environ. Microbiol.* **2004**, *70*, 4151−4157.
(10) Cheng, S. S.; Scherson, D. A.; Sukenik, C. N. In situ attenuated total reflectance fourier transform infrared spectroscopy of carboxylate-bearing, siloxane anchored, self-assembled monolayers: A study of carboxylate reactivity and acid−base properties. *Langmuir* **1995**, *11*, 1190−1195.
(11) Wasserman, S. R.; Tao, Y.-T.; Whitesides, G. M. Structure and reactivity of alkylsiloxane monolayers formed by reaction of alkyltrichlorosilanes on silicon substrates. *Langmuir* **1989**, *5*, 1074.
(12) Faucheux, N.; Tzoneva, R.; Magel, M.-D.; Groth, R. The dependence of fibrillar adhesions in human fibroblasts on substratum chemistry. *Biomaterials* **2006**, *27*, 234−245.
(13) Fryxell, G. E.; Rieke, P. C.; Wood, L. L.; Engelhard, M. H.; Williford, R. E.; Graff, G. L.; Campbell, A. A.; Wiacek, R. J.; Lee, L.; Halverson, A. Nucleophilic displacements in mixed self-assembled monolayers. *Langmuir* **1996**, *12*, 5064−5075.
(14) Masson, J.-F.; Battaglia, T. M.; Davidson, M. J.; Kim, Y.-C.; Prakash, A. M. C.; Beaudoin, S.; Booksh, K. S. Biocompatible polymers for antibody support on gold surfaces. *Talanta* **2005**, *67*, 918−925.
(15) Dai, J.; Bao, Z.; Sun, L.; Hong, S. U.; Baker, G. L.; Bruening, M. L. High-capacity binding of proteins by poly(acrylic acid) brushes and their derivatives. *Langmuir* **2006**, *22*, 4274−4281.
(16) Wang, C.; Zhang, Y. Protein micropattering via self-assembly of nanoparticles. *Adv. Mater.* **2005**, *17*, 150−153.
(17) Senaratne, W.; Sengupta, P.; Harnett, C.; Craighead, H.; Baird, B.; Ober, C. K. Molecular templates for bio-specific recognition by low-energy electron beam lithography. *Nanobiotechnology* **2005**, *1*, 23−34.
(18) Gómez, R.; Bashir, R.; Sarikaya, A.; Ladisch, M. R.; Sturgis, J.; Robinson, J. P.; Geng, T.; Bhunia, A. K.; Apple, H. L.; Wereley, S. Microfluidic biochip for impedance spectroscopy of biological species. *Biomed. Microdevices* **2001**, *3*, 20l−209.
(19) Gómez, R.; Bashir, R.; Bhunia, A. K. Microscale electronic detection of bacterial metabolism. *Sens. Actuators, B* **2002**, *86*, 198−208.
(20) Boukherroub, R.; Wojtyk, J. T. C.; Wayner, D. D. M.; Lockwoodb, D. J. Thermal hydrosilylation of undecylenic acid with porous silicon. *J. Electrochem. Soc.* **2002**, *149*, H59−H63.
(21) Voicu, R.; Boukherroub, R.; Bartzoka, V.; Ward, T.; Wojtyk, J. T. C.; Wayner, D. D. M. Formation, characterization, and chemistry of undecanoic acid-terminated silicon surfaces: Patterning and immobilization of DNA. *Langmuir* **2004**, *20*, 11713−11720.
(22) Asanuma, H.; Lopinski, G. P.; Yu, H.-Z. Kinetic control of the photochemical reactivity of hydrogen-terminated silicon with biofunctional molecules. *Langmuir* **2005**, *21*, 5013−5018.
(23) Asanuma, H.; Noguchi, H.; Uosaki, K.; Yu, H.-Z. Structure and reactivity of alkoxycarbonyl (ester)-terminated monolayers on silicon: Sum frequency generation spectroscopy. *J. Phys. Chem. B* **2006**, *110*, 4892−4899.
(24) Hyun, J.; Ma, H.; Banerjee, P.; Cole, J.; Gonsalves, K.; Chilkoti, A. Micropatterns of a cell-adhesive peptide on an amphiphilic comb polymer film. *Langmuir* **2002**, *18*, 2975−2979.
(25) Ostuni, E.; Chapman, R. G.; Holmli, R. E.; Takayama, S.; Whitesides, G. M. A survey of structure−property relationships of surfaces that resist the adsorption of proteins. *Langmuir* **2001**, *17*, 5605−5620.
(26) Sharma, S.; Johnson, R. W.; Desai, T. A. XPS and AFM analysis of antifouling PEG interfaces for microfabricated silicon biosensors. *Biosens. Bioelectron.* **2004**, *20*, 227−239.
(27) Herrwerth, S.; Eck, W.; Reinhardt, S.; Grunze, M. Factors that determine the protein resistance of oligoether self-assembled monolayers—Internal hydrophilicity, terminal hydrophilicity, and lateral packing density. *J. Am. Chem. Soc.* **2003**, *125*, 9359−9366.
(28) Bhatnagar, P.; Mark, S. S.; Kim, I.; Chen, H.; Schmidt, B.; Lipson, M.; Batt, C. A. Dendrimer-scaffold-based electron-beam patterning of biomolecules. *Adv. Mater.* **2006**, *18*, 315−319.
(29) Katz, J. S.; Doh, J.; Irvine, D. J. Composition-tunable properties of amphiphilic comb copolymers containing protected methacrylic acid groups for multicomponent protein patterning. *Langmuir* **2006**, *22*, 353−359.
(30) López, G. P.; Biebuyck, H. A.; Härter, R.; Kumar, A.; Whitesides, G. M. Fabrication and imaging of two-dimensional patterns of proteins adsorbed on self-assembled monolayers by scanning electron microscopy. *J. Am. Chem. Soc.* **1993**, *115*, 10774−10781.
(31) Brode, P. F., III; Erwin, C. R.; Rauch, D. S.; Lucas, D. S.; Rubingh, D. N. Enzyme behavior at surfaces: Site-specific variants of subtilisin BPN′ with enhanced surface stability. *J. Biol. Chem.* **1994**, *269*, 23538−23543.
(32) Bouaidat, S.; Berendsen, C.; Thomsen, P.; Petersen, S. G.; Wolff, A.; Jonsmann, J. Micropatterning of cell and protein non-adhesive plasma polymerized coatings for biochip applications. *Lab Chip* **2004**, *4*, 632−637.
(33) Lahiri, J.; Ostuni, E.; Whitesides, G. M. Patterning ligands on reactive SAMs by microcontact printing. *Langmuir* **1999**, *15*, 2055−2060.
(34) Ruiz-Taylor, L. A.; Martin, T. L.; Zaugg, F. G.; Witte, K.; Indermuhle, P.; Nock, S.; Wagner, P. Monolayers of derivatized poly(L-lysine)-grafted poly(ethylene glycol) on metal oxides as a class of biomolecules interfaces. *Proc. Natl. Acad. Sci. U.S.A.* **2001**, *98*, 852−857.
(35) Sorribas, H.; Padeste, C.; Tiefenauer, L. Photolithographic generation of protein micropatterns for neuron culture applications. *Biomaterials* **2002**, *23*, 893−900.
(36) Lee, L. M.; Heimark, R. L.; Guzman, R.; Baygents, J. C.; Zohar, Y. Low melting point agarose as a protection layer in photolithographic patterning of aligned binary proteins. *Lab Chip* **2006**, *6*, 1080−1085.
(37) Jun, Y.; Cha, T.; Guo, A.; Zhu, X.-Y. Patterning protein molecules on poly(ethylene glycol) coated Si(111). *Biomaterials* **2004**, *25*, 3503−3509.
(38) Delamarche, E.; Bernard, A.; Schmid, H.; Michel, B.; Biebuyck, H. Patterned delivery of immunoglobulins to surfaces using microfluidic networks. *Science* **1997**, *276*, 779−781.
(39) Patel, N.; Sanders, G. H. W.; Shakesheff, K. M.; Cannizzaro, S. M.; Daviews, M. C.; Langer, R.; Roberts, C.; Tendler, S. J. B.; Williams, P. M. Atomic force microscope analysis of highly defined protein patterns formed by microfluidic networks. *Langmuir* **1999**, *15*, 7252−7257.
(40) Zhang, G. J.; Tanii, T.; Zako, T.; Hosaka, T.; Miyake, T.; Kanari, Y.; Funatsu, T.; Ohdomari, I. Nanoscale patterning of protein using electron beam lithography of organosilane self-assembled monolayers. *Small* **2005**, *1*, 833−837.
(41) Kumar, N.; Hahm, J. Nanoscale protein patterning using self-assembled diblock copolymers. *Langmuir* **2005**, *21*, 6652−6655.
(42) The pK_a of MES is 6.269 at 25 °C. Roy, R. N.; Moore, C. P.; Carlsten, J. A.; Good, W. S.; Harris, P.; Rook, J. M.; Roy, L. N.; Kuhler, K. M. Second dissociation constant of two substituted aminomethanesulfonic acids in water from 5 to 55 °C. *J. Solution Chem.* **1997**, *26*, 1209−1216.
(43) Ramakrishnan, A.; Dhamodharan, R.; Rühe, J. Controlled growth of PMMA brushes on silicon surfaces at room temperature. *Macromol. Rapid Commun.* **2002**, *23*, 612−616.
(44) Coessens, V.; Pintauer, T.; Matyjaszewski, K. Functional polymers by atom transfer radical polymerization. *Prog. Polym. Sci.* **2001**, *26*, 337−377.
(45) Wu, T.; Genzer, J.; Gong, P.; Szleifer, I.; Vlèek, P.; Šubr, V. Behavior of surface-anchored poly(acrylic acid) brushes with grafting density gradients on solid substrates. In *Polymer Brushes*; Advincula, R. C., Brittain, W. J., Caster, K. C., Rühe, J., Eds.; Wiley-VCH: Weinheim, Germany, 2004; pp 287−315.
(46) Matyjaszewski, K.; Miller, P. J.; Shukla, N.; Immaraporn, B.; Gelman, A.; Luokala, B. B.; Siclovan, T. M.; Kickelbick, G.; Vallant, T.; Hoffmann, H.; Pakula, T. Polymers at interfaces: Using atom transfer radical polymerization in the controlled growth of homopolymers and block copolymers from silicon surfaces in the absence of untethered sacrificial initiator. *Macromolecules* **1999**, *32*, 8716−8724.
(47) Kurosawa, S.; Aizawa, H.; Talib, Z. A.; Atthoff, B.; Hilborn, J. Synthesis of tethered-polymer brush by atom transfer radical polymerization from a plasma-polymerized-film-coated quartz crystal microbalance and its application for immunosensors. *Biosens. Bioelectron.* **2004**, *20*, 1165−1176.
(48) Treat, N. D.; Ayres, N.; Boyes, S. G.; Brittain, W. J. A facile route to poly(acrylic acid) brushes using atom transfer radical polymerization. *Macromolecules* **2006**, *39*, 26−29.
(49) Ashford, E. J.; Naldi, V.; O'Dell, R.; Billingham, N. C.; Armes, S. P. First example of the atom transfer radical polymerisation of an acidic monomer: Direct synthesis of methacrylic acid copolymers in aqueous media. *Chem. Commun.* **1999**, *14*, 1285−1286.
(50) Osborne, V. L.; Jones, D. M.; Huck, W. T. S. Controlled growth of triblock polyelectrolyte brushes. *Chem. Commun.* **2002**, *17*, 1838−1839.
(51) The binding energy of the Na^+ 1s electron is expected to be about 1072.2 eV. Hammond, J. S.; Holubka, J. W.; Devries, J. E.; Dickie, R. A. The application of X-ray photoelectron spectroscopy to a study of interfacial composition in corrosion-induced paint deadhesion. *Corros. Sci.* **1981**, *21*, 239.

(52) The binding energies of photoelectrons from CuBr and $CuBr_2$ are reported in the NIST X-ray Photoelectron Spectroscopy Database, version 3.4, compiled and evaluated by Wagner, C. D., Naumkin, A. V., Kraut-Vass, A., Allison, J. W., Powell, C. J., and Rumble, J. R. and available online at http://srdata.nist.gov/xps.
(53) Husemann, M.; Morrison, M.; Benoit, D.; Frommer, J.; Mate, C. M.; Hinsberg, W. D.; Hedrick, J. L.; Hawker, C. J. Manipulation of surface properties by patterning of covalently bound polymer brushes. *J. Am. Chem. Soc.* **2000**, *122*, 1844−1845.
(54) Beamson, G.; Briggs, D. *High Resolution XPS of Organic Polymers: The Scienta ESCA300 Database*; John Wiley & Sons: Chichester, U. K., 1992.
(55) High ionic strength solution is expected to result in desorption of the physically adsorbed protein. Wittemann, A.; Haupt, B.; Ballauf, M. Adsorption of protein on spherical polyelectrolyte brushes in aqueous solution. *Phys. Chem. Chem. Phys.* **2003**, *5*, 1671−1677.
(56) Wissink, M. J. B.; Beernink, R.; Pieper, J. S.; Poot, A. A.; Engbers, G. H. M.; Beugeling, T.; van Aken, W. G.; Feijen, J. Immobilization of heparin to EDC/NHS-crosslinked collagen. Characterization and in vitro evaluation. *Biomaterials* **2001**, *22*, 151−163.
(57) Patrickios, C. S.; Yamasaki, E. N. Polypeptide amino acid composition and isoelectric point. *Anal. Biochem.* **1995**, *231*, 82−91.
(58) Rao, S. V.; Anderson, K. W.; Bachas, L. G. Oriented immobilization of proteins. *Mikrochim. Acta.* **1998**, *128*, 127−143.
(59) Rao, S. V.; Anderson, K. W.; Bachas, L. G. Controlled layer-by-layer immobilization of horseradish peroxidase. *Biotechnol. Bioeng.* **1999**, *65*, 389−396.
(60) Hiller, Y.; Gershoni, J. M.; Bayer, E. A.; Wilchek, M. Biotin binding to avidin. *Biochem. J.* **1987**, *248*, 167−171.
(61) Nehilla, B. J.; Popat, K. C.; Vu, T. Q.; Chowdhury, S.; Standaert, R. F.; Pepperberg, D. R.; Desai, T. A. Neurotransmitter analog tethered to a silicon platform for neuro-BioMEMS applications. *Biotechnol. Bioeng.* **2004**, *87*, 669−674.
(62) De Lange, R. J.; Huang, T.-S. Egg white avidin. *J. Biol. Chem.* **1971**, *246*, 698−709.
(63) Bruch, R. C.; White, H. B., III. Compositional and structural heterogeneity of avidin glycopeptides. *Biochemistry* **1982**, *21*, 5334−5341.
(64) Bomben, K. D.; Dev, S. B. Investigation of poly(L-amino acids) by X-ray photoelectron spectroscopy. *Anal. Chem.* **1988**, *60*, 1393−1397.
(65) Amino acid residues with aromatic rings are expected to show shakeup satellite peaks due to $\pi \rightarrow \pi^*$ excitation of the valence electrons. The shakeup satellite peak is usually seen near 291 eV for phenyl rings. Bomben and Dev have reported that, in the cases of phenylalanine, tryptophan, and tyrosine, the intensity of the shakeup satellite was bout 2% of the total carbon intensity.[64] These residues contribute to only about 17.5% of the carbon atoms in avidin, so the intensity of the shakeup satellites would be less than 0.5% of the total carbon intensity. As such, no satellite peaks were observed near 291 eV.
(66) In addition to lysine, arginine, and proline, each of which contains one carbon of the C−N type (per residue), curve fitting indicated that the α-carbon atoms along the protein backbone also contributed to the C−N peak. All of the carbon atoms in the phenyl group of phenylalanine, the indole group of tryptophan, and the phenol group of tyrosine were considered to be of the hydrocarbon type, in accordance with the analysis of Bomben and Dev.[64] The carbon atoms in the imidazole group of histidine were similarly reckoned as C−C carbon atoms. The carboxylic C═O carbon atoms are expected from the aspartic acid and glutamic acid residues in avidin. However, we did not attempt to determine the percentage of PAA carboxylic acid groups that have reacted with the avidin amine groups. The number of amide linkages so formed will be small in comparison to the amide carbon atoms of the protein backbone, and the curve-fitting analysis is not sensitive enough to detect such small differences.
(67) Ebersole, R. C.; Miller, J. A.; Moran, J. R.; Ward, M. D. Spontaneously formed functionally active avidin monolayers on metal surfaces: A strategy for immobilizing biological reagents and design of piezoelectric biosensors. *J. Am. Chem. Soc.* **1990**, *112*, 3239−3241.
(68) Tan, Z.; Xia, Y.; Zhao, M.; Liu, X. Electron stopping power and inelastic mean free path in amino acids and protein over the energy range of 20−20,000 eV. *Radiat. Environ. Biophys.* **2006**, *45*, 135−143.
(69) To estimate the percentage contribution of the avidin monolayer to the C 1s peak area, a two-layer model was assumed wherein the top avidin monolayer, with a thickness of 4.8 nm, completely covers the bottom layer of pure PAA. For electron emission along the surface normal, the intensity of photoelectrons originating from a surface layer with a thickness, d, of 4.8 nm (and hence from the avidin layer) is given by $1 - \exp(-d/\lambda)$, where λ is the electron escape depth. The inelastic mean free path (IMFP) of the electron at a kinetic energy of about 1200 eV (close to kinetic energy of C 1s photoelectrons) was used as an estimate of the electron escape depth. The IMFP of electrons in protein was obtained from ref 68. It should be noted that the IMFP of an electron in PAA is quite similar (∼3.2 nm).
(70) Czeslik, C.; Jackler, G.; Steitz, R.; von Grünberg, H.-H. Protein binding to like-charged polyelectrolyte brushes by counterion evaporation. *J. Phys. Chem. B* **2004**, *108*, 13395−13402.
(71) Rosenfeldt, S.; Wittemann, A.; Ballauff, M.; Breininger, E.; Bolze, J.; Dingenouts, N. Interaction of proteins with spherical polyelectrolyte brushes in solution as studied by small-angle X-ray scattering. *Phys. Rev. E* **2004**, *70*, 61403.
(72) From angle-resolved XPS studies of BSA immobilized on PAA brushes (cf. Scheme 3), the protein molecules could be detected up to a depth of several nanometers below the brush surface. The number fraction of BSA carbon atoms in the thin film decreased from about 80% at the surface to less than 10% within 15 nm of depth. A detailed analysis will be presented in a separate report.
(73) Lee, M. H.; Brass, D. A.; Morris, R.; Composto, R. J.; Ducheyne, P. The effect of non-specific interactions on cellular adhesion using model surfaces. *Biomaterials* **2005**, *26*, 1721−1730.

BM700493V